International Journal of Advanced Technology and Innovative Research

www.ijatir.org

ISSN 2348–2370
Vol.09,Issue.04,
March-2017,
Pages:0547-0553

Aerodynamic Effect Caused by Ice Aircraft Wing

N. RAMAKRISHNA[1], V. PRADEEP KUMAR[2]

[1]PG Scholar, Dept of Mechanical, Gokul Group of Institutions, Bobbili, Vizianagaram, AP, India.
[2]Associate Professor, Dept of Mechanical, Gokul Group of Institutions, Bobbili, Vizianagaram, AP, India.

Abstract: Past exploration on airfoil and wing optimal design in icing are looked into. This survey stresses the time period after the 1978 NASA Lewis workshop that started the advanced icing examination program at NASA and the ebb and flow period after the 1994 ATR mischance where optimal design exploration has been more flying machine security centered. Research pre-1978 is likewise quickly assessed. Taking after this audit, our present information of frosted airfoil streamlined features is introduced from a flowfield-material science viewpoint. This article recognizes four classes of ice gradual additions: harshness, horn ice, stream shrewd ice, and compass insightful edge ice. For every class, the key flowfield elements, for example, flowfield division and reattachment are examined and how these add to the known streamlined impacts of these ice shapes. At last Reynolds number and Mach number consequences for frosted airfoil streamlined features are outlined.

Keywords: Aerodynamics, Flow Physics, Airfoils, Aircraft Icing, Performance Degradation, Mach Number, Rime, Glaze, SLD, Roughness, Lift, Drag.

I. INTRODUCTION

Plane amid flight. Accumulated ice antagonistically influences flight; along these lines, it is a vital segment to fan avionics climate conjecture. Meteorology related inside of flight icing starts with the miniaturized scale, tending to development of super cooled beads and their impact with and bond to airframes. Cloud-scale and mesoscale procedures control the sum and dissemination of super cooled fluid water. Concise climate examples administer the development and general area of icing situations. Any talk of flying machine icing must additionally incorporate the improvement and utilization of numerical climate expectation models and demand and remote sensors for icing recognition, Analysis, and estimating. There are disengaged instances of snow and ice grip amid flight, yet since these infrequently happen they won't be talked about here. Additionally, precipitation or ice holding fast to the wings of a plane preceding departure, and carburetor icing, won't be secured. Icing examination started in the late 1920s and mid-30s, however it wasn't until WWII that icing passages were fabricated and icing was genuinely tended to in light of the war exertion. From this time until the begin of the cutting edge icing examination program in 1978 at NASA Glenn (then Lewis) Research Center, the center of streamlined exploration was to quantify the impact of ice on the lift and drag of airfoils or the general air ship execution parameters.

This was compressed by the Gray connection [1] for frosted airfoil drag in 1964 and the surely understood plot of Brumby [2] in 1979 that incorporated the known information of the opportunity to introduce experimental bends of most extreme lift misfortune versus unpleasantness size and area. With the NASA flying machine icing program that was started in 1979, Computational Fluid Dynamics (CFD) started to be created and connected to the forecast of streamlined execution of airfoils with ice. To bolster this work, frosted airfoil streamlined features examination was started to give nitty gritty streamlined information to use in code approval and trial results including the first stream field estimations. This started to show up in the writing in the mid-1980s. These information, and the comparing CFD computations, gave the first look of the stream material science of frosted airfoil optimal design. Ice-instigated detachment air pockets were found to rule the stream field and the streamlined execution in numerous imperative cases. In 1994 the Roselawn ATR-72 mischance strengthened the significance of icing optimal design look into and changed its center from an experimental activity to one obviously centered around air ship wellbeing. This included propelling the exploratory and computational examination of diverse sorts of ice gradual additions including Super cooled Large-Droplet (SLD) shapes and intercycle ice shapes.

Somewhat in light of the requirement for better criteria for selecting "basic ice shapes," the absolute most point by point parametric investigations of ice shape and airfoil geometry impacts on airfoil and wing streamlined features have as of late been finished. Huge understanding has been picked up into frosted airfoil and wing optimal design measurements obtained in the 1940s and is illustrated in Fig.1, which was designed to envelop 99.9% of icing conditions found. The shaded areas denote the limits of these environmental parameters in which aircraft must be able to fly safely to be certified for flight into icing conditions. Icing tends to affect general aviation less than commuter or air carrier operations; there are several reasons for this. The smaller aircraft included in the general aviation category tend to fly at lower altitudes where icing is more prevalent. Those aircraft may have less de-icing capability and reserve

power in case of encountering icing conditions, and their pilots may have less experience of operating under icing conditions. Air carriers tend to quickly penetrate icing bearing clouds on ascent and descent from airports and cruise at altitudes far above those at which icing occurs. Commuter aircraft are caught in the middle, in terms of both their ability to handle ice and the altitudes at which they fly. With the burgeoning business in this area, they find themselves susceptible to icing and need accurate forecasts.

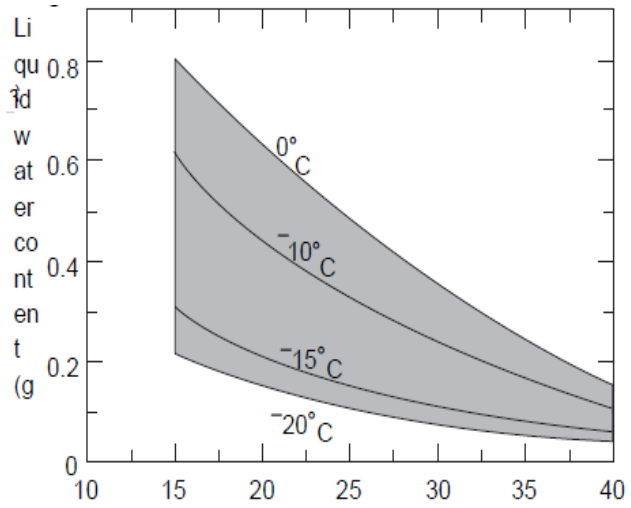

Fig.1. Icing envelopes defined by liquid water content, droplet size, and temperature.

III. TYPES OF ICING

There are two main physical types of icing: glaze and rime. Mixed icing is a combination of the two. Rime ice is brittle and opaque and tends to grow into the airstream. It is formed as the droplets freeze immediately upon impact. Glaze icing, sometimes referred to as clear icing, can be nearly transparent and has a smoother surface, sometimes with a waxy appearance as shown in Fig.2. It is formed when the droplets deform and/or flow along the surface prior to freezing. Glaze icing can be more serious to the aircraft than rime since it tends to run back along the airframe, covering more surface area than rime icing F perhaps flowing onto and adhering to unprotected areas. Glaze icing can be hard to see from inside the aircraft, so that the pilot may be unaware of ice buildup. Mixed icing often occurs in layers, similar to wet and dry hailstone 0.8 growth, as a transition from rime to clear conditions is encountered. The leading edge of the left wing is shown in each photograph: (A) light rime ice, (B) severe glaze ice, (C) moderate mixed ice, (D) super cooled large droplet ice. Note how much farther aftthe ice in (D) has accreted compared to the other types. (Photographs courtesy of NASA Glenn Research Center.) The type of icing is related to the air temperature, the liquid water content, and the size of the droplets. Glaze is generally associated with higher temperatures, higher super cooled liquid water (SLW) contents and larger droplets. Rime is usually created at lower temperatures, low SLW contents and small droplet size. There are also effects dependent on the airplane itself, including wing shape, airspeed, and type of deicing/anti-icing equipment.

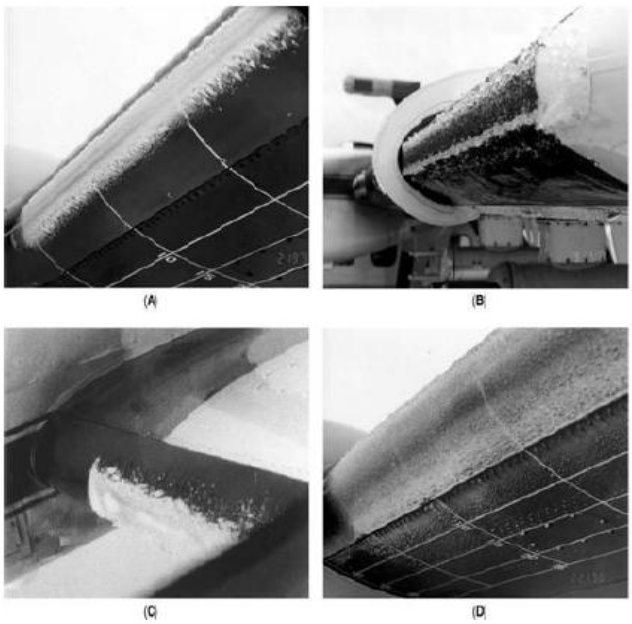

Fig.2. Post-flight photographs of ice encountered by the NASA Glenn Research Center's instrumented Twin Otter aircraft.

IV. LOCATION AND FREQUENCY OF ICING CONDITIONS

Since icing occurs in clouds or precipitation at temperatures below 01C, any icing climatology must be associated with cold, cloudy conditions. Figure 3 shows that icing frequency is most strongly related to latitude in the contiguous United States, with some preference for the northeastern part of the country. Icing-related fatal aircraft accidents average approximately 30 per year in the United States, with the highest incidence in the winter months. Alaska has by far the highest accident rate, followed by the northwest mountains, Great Lakes, western Pacific states and the central states. The average altitude of icing environments is around 3000m above mean sea level (msl), with few encounters above 6000m. Cumuliform clouds, with their greater depth and transport of significant liquid amounts to higher altitudes, have on average higher altitude coverage than strati form clouds. Frequency of icing 'PIREPs' (pilot reports) by time of day is a direct reflection of the frequency of flights, with few reports overnight. The weekly pattern also follows air traffic trends, with most reports on Tuesday through Thursday. Light icing is the most frequent severity category reported by pilots, accounting for B60–70% of all reports. Severe icing, which indicates a condition in which flight cannot be sustained, is reported in only a few percent of cases. Rime icing is reported much more frequently than glaze or mixed, comprising B70–75%ofreports. For both icing type and severity, the largest joint frequency is for light rime icing, which covers nearly half of all reports.

V. ICED AIRFOIL AERODYNAMICS

Based on the detailed aerodynamic measurements taken on iced airfoils and wings since 1978, and primarily since 1995, this section presents the current understanding of these flowfields. This discussion is divided into four parts based

on representative ice geometries: 1) roughness, 2) horn ice, 3) streamwise ice, and 4) spanwise-ridge ice. Of course many ice shapes are not purely one or the other of these shapes, but may have features representative of two or more of these types. Fig. 3 qualitatively shows the four types of ice shapes with the vertical axis representing increased two-dimensionality and the horizontal axis representing increasing flow disturbance (and therefore degradation in aerodynamic performance). Roughness is in the lower left corner as the most 3D shape with low to moderate disturbance of the flowfield. Streamwise, horn, and spanwise-ridge ice are all more 2D and have increasing aerodynamic effect from streamwise ice with the least to spanwise ridge with the largest effect. The circles representing the different shapes overlap representing the fact that some shapes have characteristics of more than one type. The characteristics of these four types of ice are explained in the sections that following Fig.3.

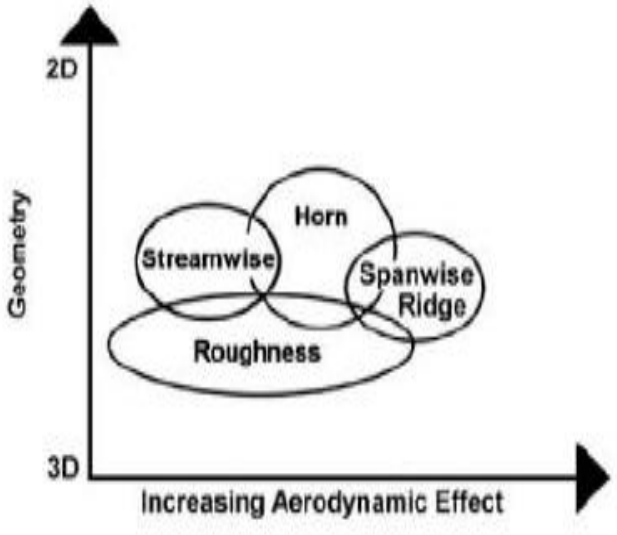

Fig.3. Qualitative description of aerodynamic effects for various iced-airfoil flowfields.

VI. ICE ROUGHNESS

Ice roughness occurs during the initial stages of the ice accretion process before a significant ice shape, such as a horn, is accreted. The other three ice types are also "rough," but here we focus on the initial surface roughness due to ice before accretion has significantly altered the airfoil contour and thus the inviscid flowfield. In a study by Shin [68] and Anderson and Shin [69] the characterization of ice roughness was investigated. They found that three main zones evolve on the leading edge in glaze and rime ice conditions— the smooth zone, rough zone, and feather region (Fig. 4). The height and diameter of the roughness elements that occur in each zone are dependent on the associated freezing fraction and accumulation parameter. Ice roughness may also occur due to feather formation, ice protection system operation, etc. For aircraft components operating at typical Reynolds numbers, ice roughness is of a height greater than the local boundary-layer thickness, even at the very early stages of development. Shin [68] measured bead heights from 0.28 – 0.79 mm, much thicker than the expected local boundary layer. Measurements on other types of ice roughness from feathers to residual ice are also generally large when compared to the local boundary layer thickness. This, of course, influences how the ice roughness affects the boundary-layer development and ultimately the aerodynamic performance. For ice roughness greater than the boundary-layer thickness, and low roughness density, each roughness element acts as its own isolated body. This situation is often referred to in the aerodynamic literature as a flow obstacle. These roughness elements are bluff bodies with 3D separation behind each element with the characteristic length of the separation on the order of the roughness size. The element drag and the separation govern the effect the roughness has on the airfoil flowfield and boundary-layer development. The boundary between roughness and an ice feature, such as a horn, is not always clear as indicated by the overlapping of the two ice types as shown in Fig.4.

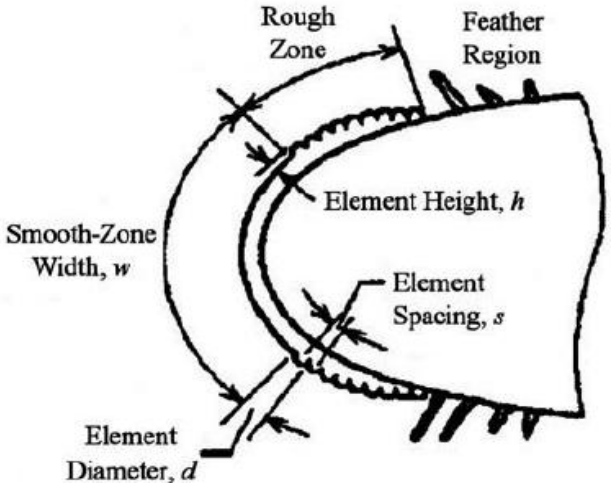

Fig.4. Ice roughness features.

One distinction is in the nature of the flow separation generated by the shape. As will be described in a later section, an ice horn produces a primarily 2D separation region aft of the horn. Here we consider roughness as a primarily 3D shape that produces local 3D separation behind elements while horn ice (or for that matter spanwise ridge ice) generates primarily 2D separation with separation lengths and widths large compared to the characteristic height of the ice feature. Roughness is characterized by its height, density, and surface location. The effect on airfoil performance is dependent on all these parameters. Roughness shape can also be significant, but of the irregular shapes seen in ice roughness it is not thought to be as important, and is certainly less well understood, than the other three parameters for ice roughness. Roughness affects airfoil or wing performance by first directly increasing the skin friction. Roughness can also cause early boundary layer transition and promote thickening of the boundary layer leading to early trailing-edge separation. These effects then manifest themselves through modified skin friction and pressure distributions into performance degradation. The effect of initial isolated and distributed ice roughness on boundary-layer transition was studied in detail by Kerhoand Cummings. Kerho carefully studied the boundary-layer

development on an airfoil with simulated ice roughness at various locations on the leading edge. Here transition is initiated by the complex local flowfield of the element and is called bypass transition, since it bypasses the classic Tollmien-Schlicting mechanism.

Unlike natural transition which occurs suddenly and energetically, this research showed that roughness initiated a transitional boundary layer which slowly transitioned to a turbulent boundary layer. This process appeared to depend on the local pressure gradient. The boundary layer transition due to a single element was observed by Cummings to depend on the roughness Reynolds number Rek = ρukk/μ (Fig. 3). The dependence on Rek is shown in Fig. 4. When Rek was much less than the critical Reynolds number, no transition wedge was seen. As Rek increased closer to Rek,crit, the transition wedge appeared downstream of the element. When Rek was further increased, the transition wedge approached the element. However, Cummings emphasizes that while the term Rek,crit is used to represent turbulence occurring at the element, when k/δ is greater than one, the transition actually moves rapidly toward the element while not actually reaching the element. When the element is located on an airfoil, it is also important to consider the local pressure gradient. Cummings found that depending on k/δ and the local pressure gradient, multiple Rek,crit values exist. Fig.5 represents the qualitative flowfield about a hemisphere for an Rekof 300. In this regime the flow is stable and does not create a turbulent wedge downstream. From Fig. 5, the incoming streamline can be seen to come to a stagnation point on the surface of the element.

As fluid close to the wall approaches the element, an adverse gradient causes the incoming fluid to form the primary vortex shown. The primary vortex wraps around the element forming the horseshoe vortex system. As Re increases, the rear separation pocket becomes unstable and an onset of turbulence appears in the form of a turbulent wedge. While a value of approximately 600 is usually used to denote Rek,crit. Cummings and Bragg [72] observed a dramatic increase in the leading edge region to values approaching 2000. This was thought to be due to increased stability of the boundary layer in this region and the very favorable pressure gradient as shown in Fig.6.

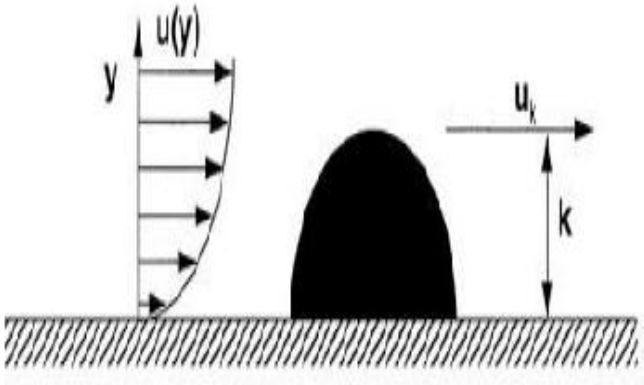

Fig.5.Definition of roughsnse height(k) and velocikt).y(u).

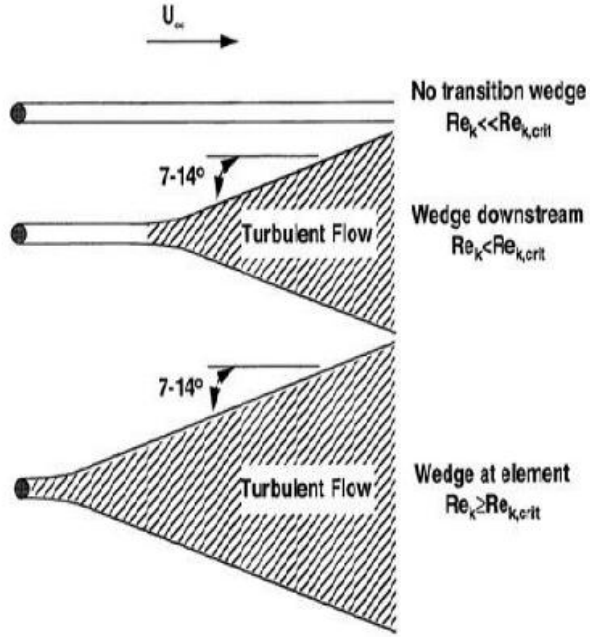

Fig.6. Three dimensionalu rgohness transition wedges.

VII. HORN ICE

The horn shape can be characterized by its height, the angle it makes with respect to the chord line (θ), and its location indicated by s/c, the no dimensional surface length, a horn ice accretion is shown with both an upper and lower horn. Much of the parametric research conducted to date on horn ice has only considered a single horn. The discussion in this section will address the effects of a single horn first, as this feature controls the flowfield, then briefly review some results with single and double horn simulations. Horn ice is usually produced in glaze ice conditions and the horn geometry sketched below is normally part of a larger accretion that may also include feather formations downstream of the horns. In Fig. 7 the horn shape is shown as more 2D than surface roughness and with a larger aerodynamic effect than stream wise ice, but less than span wiseridge ice.

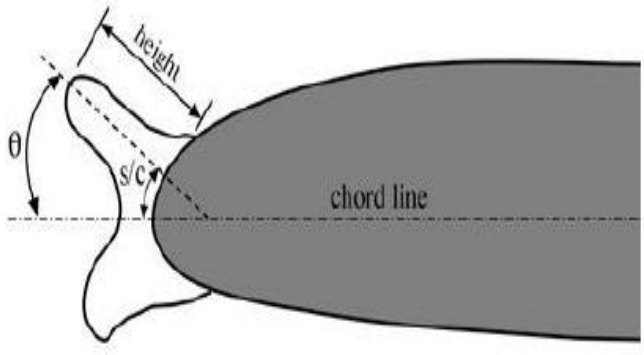

Fig.7. Geometry of a horn ice shape.

The dominant flow feature that determines the aerodynamics of an airfoil with a horn ice shape is the separation bubble that forms downstream of the horn. This bubble is similar to the long bubble as defined by Tani in

that it has a global effect on the airfoil pressure distribution. Laminar separation bubbles that form on clean airfoils have been widely studied and much is known about their characteristics. There are a number of similarities to the separation bubbles that result from horn ice shapes on airfoils. A sketch of a laminar separation bubble, adapted from Roberts, is shown in Fig. along with the accompanying pressure distribution. On clean airfoils, the bubble forms when the laminar boundary layer encounters an adverse pressure gradient of sufficient strength to cause separation at point S in Fig.8. On iced airfoils, the boundary layer separates near the top of the horn, due to the pressure gradient produced by the large discontinuity in the surface geometry. In both cases, the separation leads to the formation of a shear layer over the bubble and characteristic flow reversal near the surface. At point T, the shear layer transitions to turbulent flow. The static pressure in the bubble is seen to be fairly constant over the bubble until transition. After transition, the magnitude of the reverse flow increases and a vortex type flow is seen in the bubble.

As the turbulent shear layer entrains high energy external flow, pressure recovery becomes possible and the bubble reattaches at point R. In the icedairfoil case, the shear-layer transition process is likely less energetic than this discussion would imply. The transitional flow was discussed in the section on Ice Roughness. Despite this, the iced-induced separation bubbles contain many similarities to Fig. An understanding of the separation bubble flowfield is critical to understanding the horn-ice effects on airfoil performance. Nearly all of the integrated effects can be interpreted in terms of the separation bubble behavior. Most flowfield studies of these separation bubbles focused on the time-averaged characteristics. However, the bubble flowfields are known to have strong unsteady characteristics that also play a role in the aerodynamics. These unsteady features are discussed after the time-averaged characteristics.

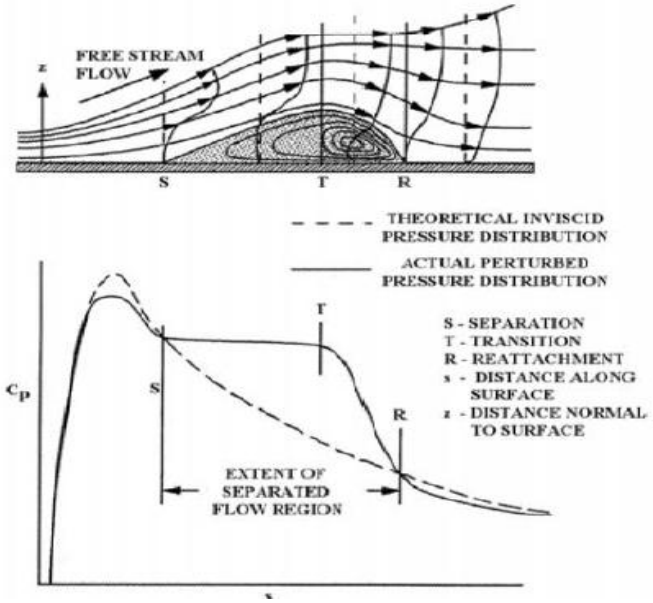

Fig.8. Laminar separation bubble schematic and characteristic pressure distribution, adapted from Roberts.

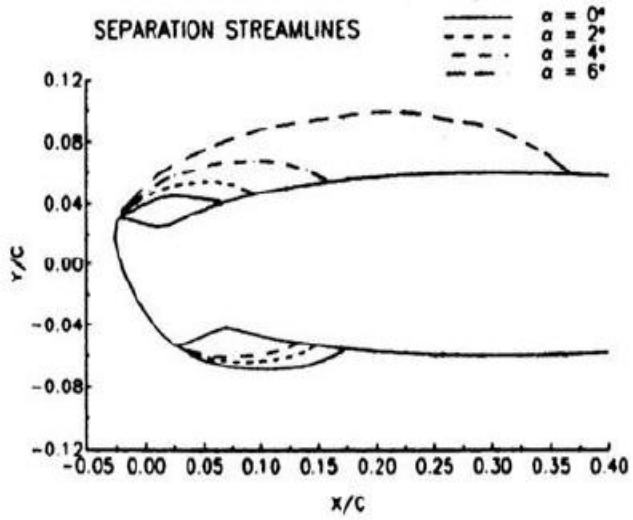

Fig.9. Separation streamlines with angle of attack for a NACA 0012 airfoil with simulated horn ice accretion, Re = 1.5×106, M = 0.12.

Bragg, Khodadoust, and Spring studied the time averaged flowfield due to a simulated 5-minute glaze ice shape on a NACA 0012 using split-film anemometry. Figure shows the upper and lower surface separation streamlines, calculated from the measured velocity field, for separation bubbles for four different angles of attack as shown in Fig.9. This horn shape caused bubbles to form on both the upper and lower surface. The separation streamline is the streamline in the shear layer that divides fluid that recirculates from fluid that flows over the separation bubble and downstream in a time-averaged view of the flowfield. The upper surface separation bubble caused by the ice was seen to increase in size as the angle of attack was increased until the bubble failed entirely to reattach ($\alpha > 6$ deg.), and the airfoil upper surface was completely separated in a steady-state model. The streamlines show that the boundary-layer separation point was fixed near the tip of the simulated ice horn for all angles of attack. The increase in bubble size resulted in increasing drag and the airfoil stalled when the bubble failed to reattach. The pressure distribution corresponding to the $\alpha = 4$ deg. case with and without simulated ice is shown. For the iced case the pressure is seen to be relatively constant from the leading edge to x/c = 0.10 on the upper surface.

As discussed in terms of the laminar separation bubble, this is indicative of a separation bubble over this region. The "Transition" and "Reattachment" labels are based on Tani's definition as discussed in connection with Fig. 10. Aft of x/c = 0.10 the pressure increases (Cp becomes more positive) as the bubble starts to reattach. The reattachment location occurred near the location where the clean and iced pressure distributions intersect on the upper and lower surface. (The bubble on the lower surface, indicated by the pressure plateau, was due to the lower surface horn.) This location is consistent with that measured by Bragg et al. The method of approximating the bubble reattachment location as the intersection of the clean and iced pressure distributions was

investigated by Bragg et al. and was found to be accurate for the ice shape tested.

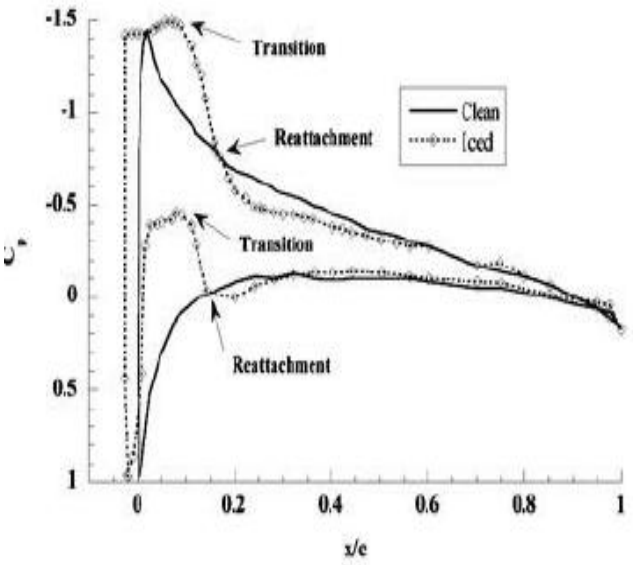

Fig.10. Surface pressure distribution for a NACA 0012 airfoil with and without simulated horn ice accretion, α = 4 deg., Re = 1.5×106, M = 0.12, adapted from Bragg, Khodadoust, and Spring.

VIII. CONCLUSION

This paper presents a brief review Performance of Ice Aircraft wing and icing aerodynamics research as well as the flowfield and aerodynamics of airfoils with simulated ice accretions. Icing research began in the late 1920s and early 1930s in order to measure the effect of ice on the overall performance parameters of airfoils, such as the lift and drag. It was not until the NASA aircraft-icing program, initiated in 1979, that detailed flowfield measurements were performed. This research was originally performed to obtain data to validate the results of CFD calculations focusing on a small subset of ice shapes. The Roselawn ATR-72 accident in 1994 broadened the focus of aerodynamic research to include "critical ice-shape" initiatives along with the consideration of different airfoil effects and other related issues. In this paper the key flowfield features that dominate the flow physics were examined. The ice accretions were divided into four main categories in order to describe the different flow physics and aerodynamic effects. However, it is important to note that many ice shapes cannot simply be categorized into just one group. An ice shape may have characteristics of several categories. By breaking down a complicated ice shape, the expected flow features and important aerodynamic effects can be determined. In addition, ice accretions in a given category are not all identical and can exhibit different characteristics depending on their shape and the airfoil geometry. The four categories were: roughness, horn ice, streamwise ice, and span wiseridge ice. Principle findings for the four ice types were:

- Roughness effects are determined by the height, density, and surface location of the roughness elements. Most ice roughness is larger than the local boundary layer and increasing height increases the aerodynamic effect. The aerodynamic effects result not only from the influence on boundarylayer transition, but due to the size of the roughness, have a significant effect on separation downstream. The leading edge was shown to be the most critical location and concentration was important particularly at values less than 30%.
- Horn ice flowfields are characterized by large flow separation regions aft of the horn which dominate the aerodynamics. The separation location is relatively fixed by the geometry of the ice shape. These separation regions grow with angle of attack and lead to thin-airfoil type stall. Horn size, location, and angle are key parameters, with roughness and the cross-sectional geometry of the horn having much smaller effects.
- Streamwise ice forms in streamline shapes on the leading edge and thus the flow separation is less significant than for horn ice. For the more conformal streamwise ice accretions, the separation point is not fixed but varies with angle of attack and the aerodynamics are less a function of ice shape size than in the horn case. The addition of surface roughness was seen to increase the drag but have a small effect on the lift. Some streamwise accretions are less conformal and have characteristics that appear as a horn directed into the flow. For these accretions the separation point maybe relatively fixed by the geometry, but the separation bubble is small compared to the horn accretions and the aerodynamic penalties less severe as is typical of streamwise ice.
- Spanwise-ridge ice usually forms farther back on the airfoil surface than horn ice and, while there are similarities to horn ice, has a different flowfield. Spanwise-ridge ice is a flow obstacle, since the airfoil boundary layer develops along the airfoil surface before encountering the ridge. As for the horn, a potentially large separation region forms downstream of the ridge, but here a separation also forms upstream and the flowfield upstream of the ridge on the clean airfoil surface can have a large effect on the airfoil performance. Ridge location and height are key parameters, but the geometry of the ridge has also been shown to be important.

IX. REFERENCES

[1] Gray VH. Prediction of Aerodynamic Penalties Caused by Ice Formations on Various Airfoils.NASA TN D–2166, 1964.

[2] Brumby RE. Wing Surface Roughness – Cause & Effect. D.C. Flight Approach, Jan. 1979. pp. 2-7.

[3] Lynch FT, Khodadoust A. Effects of Ice Accretions on Aircraft Aerodynamics. Prog Aerospace Sci 2001; 37: 669-767.

[4] Carroll TC, McAvoy WH. Formation of Ice on Airplanes. Airway Age, Sept. 1928. pp.58-59.

[5] Jacobs EN. Airfoil Section Characteristics as Affected by Protuberances. NACA Report No. 446, 1932.

[6] Jones R, Williams DH. The Effect of Surface Roughness of the Characteristics of the Aerofoils NACA 0012 and RAF 34.British ARC, R&M No. 1708, 1936.

[7] Gulick BG. Effects of Simulated Ice Formation on the Aerodynamic Characteristics of an Airfoil. NACA Wr L-292, 1938.
[8] Johnson CL. Wing Loading, Icing and Associated Aspects of Modern Transport Design. J Aero Sci 1940; 8 (2): 43-54.
[9] Icing Research Tunnel. Program from the ASME dedication as an International Historic Mechanical Engineering Landmark, May 20, 1987.
[10] Gray VH, Von Glahn UH.Effect of Ice and Frost Formations on Drag of NACA 65-212 Airfoil for Various Modes of Thermal Ice Protection. NACA TN 2962, June 1953.
[11] Von Glahn UH, Gray VH. Effect of Ice Formations on Section Drag of Swept NACA 63A- 009 Airfoil with Partial-Span Leading-Edge Slat for Various Modes of Thermal Ice Protection. NAC RM E53J30, March 15, 1954.
[12] Bowden DT. Effect on Pneumatic De-Icers and Ice Formations on Aerodynamic Characteristics of an Airfoil. NACA TN 3564, February 1954.
[13] Gray VH, Von Glahn UH.Effect of Ice and rost Formations on Drag of NACA 65-212 Airfoil for Various Modes of Thermal Ice Protection. ACA TN 2962, June 1953.
[14] Gray VH, Von Glahn UH. Aerodynamic Effects Caused by Icing of an Unswept NACA 65A004 Airfoil. NACA TN 4155, 1957.
[15] Gray VH. Correlations Among Ice Measurements, Impingement Rates, Icing Conditions, and Drag Coefficients for Unswept NACA 65A004 Airfoil. NACA TN 4151, February 1958.

Author's Profile:

N RamaKrishna pursuing his M.Tech in the department of mechanical Engineering, specialisation in Thermal Engineering, Gokul group of Institutions, Vizainagaram, AP, India. He obtained his B.Tech(Mech) from St Ann's College of Engineering and Technology.

V. Pradeep Kumar, M Tech working as associate professor in the department of Mechanical Engineering, Gokul Group of Institutions, Vizainagaram, AP, India.